

Myeloid-Derived Suppressor Cells Infiltrate the Heart in Acute *Trypanosoma cruzi* Infection

Henar Cuervo,* Néstor A. Guerrero,*[†] Sofía Carbajosa,* Alain Beschin,^{‡,§}
Patrick De Baetselier,^{‡,§} Núria Gironès,*^{†,1} and Manuel Fresno*^{†,1}

Chagas disease, caused by the protozoan parasite *Trypanosoma cruzi*, affects several million people in Latin America. Myocarditis, observed in the acute and chronic phases of the disease, is characterized by a mononuclear cell inflammatory infiltrate. We previously identified a myeloid cell population in the inflammatory heart infiltrate of infected mice that expressed arginase I. In this study, we purified CD11b⁺ myeloid cells from the heart and analyzed their phenotype and function. Those CD11b⁺ cells were ~70% Ly6G⁻Ly6C⁺ and 25% Ly6G⁺Ly6C⁺. Moreover, purified CD11b⁺Ly6G⁻ cells, but not Ly6G⁺ cells, showed a predominant monocytic phenotype, expressed arginase I and inducible NO synthase, and suppressed anti-CD3/anti-CD28 Ab-induced T cell proliferation in vitro by an NO-dependent mechanism, activity that best defines myeloid-derived suppressor cells (MDSCs). Contrarily, CD11b⁺Ly6G⁺ cells, but not CD11b⁺Ly6G⁻ cells, expressed S100A8 and S100A9, proteins known to promote recruitment and differentiation of MDSCs. Together, our results suggest that inducible NO synthase/arginase I-expressing CD11b⁺Ly6G⁻ myeloid cells in the hearts of *T. cruzi*-infected mice are MDSCs. Finally, we found plasma L-arginine depletion in the acute phase of infection that was coincident in time with the appearance of MDSCs, suggesting that in vivo arginase I could be contributing to L-arginine depletion and systemic immunosuppression. Notably, L-arginine supplementation decreased heart tissue parasite load, suggesting that sustained arginase expression through the acute infection is detrimental for the host. This is, to our knowledge, the first time that MDSCs have been found in the heart in the context of myocarditis and also in infection by *T. cruzi*. *The Journal of Immunology*, 2011, 187: 2656–2665.

Chagas disease, which is caused by the protozoan parasite *Trypanosoma cruzi*, affects ~18 million people in Latin America, with 120 million at risk, thus remaining a major cause of morbidity and mortality in that region (1). Myocarditis that occurs as a result of infection is the most serious and frequent manifestation of chronic Chagas disease and appears in 30% of

infected individuals several years after the infection. The pathogenesis is thought to be dependent on an immune-inflammatory reaction to a low-grade infection (2, 3). *T. cruzi* has a complex life cycle involving several life stages in both vertebrates and insect vectors. It infects and replicates in macrophages and cardiomyocytes and many other cell types. Resistance to the disease is associated with a Th1 response, which efficiently controls infection through IFN- γ production and further increased activity of inducible NO synthase (iNOS; also termed NOS2), which metabolizes L-arginine (a semiessential amino acid) and produces NO (4). In addition, during acute infection, there is suppression of T cell proliferation that is partially caused by NO (5). Moreover, the development of severe cardiomyopathy in Chagas disease is also thought to be due to a Th1-specific immune response (6).

In contrast, L-arginine can also be used by arginase I, which produces ornithine that in turn is metabolized by ornithine decarboxylase to produce polyamines needed for growth of all eukaryotic cells. In this regard, arginase I expression was found to be upregulated in macrophages infected with *T. cruzi* and associated with parasite survival (7, 8).

In mice, arginase I has been described to be expressed by different myeloid cell subsets such as alternatively activated macrophages (also called M2 macrophages) and myeloid-derived suppressor cells (MDSCs), among others. Whereas M2 macrophages are thought to express arginase I but not iNOS (9), MDSCs can express both enzymes (10). M2 macrophages induced by type 2 and regulatory cytokines have been implicated in parasite growth (11) and can be defined by an M2 gene signature (12). In contrast, MDSCs accumulate during acute and chronic immune responses to pathogens, tumor growth, trauma, and other immunological responses (13). These cells are commonly identified in mice by the coexpression of CD11b and Gr-1 (Ly6G/Ly6C) surface markers. However, this population shows important phenotypic differences depending on the anatomical site where they are

*Centro de Biología Molecular Severo Ochoa, Consejo Superior de Investigaciones Científicas, Universidad Autónoma de Madrid, Cantoblanco, 28049 Madrid, Spain; [†]Instituto de Investigación Sanitaria Princesa, Hospital Universitario de La Princesa, 28006 Madrid, Spain; [‡]Department of Molecular and Cellular Interactions, Flemish Institute for Biotechnology, 1050 Brussels, Belgium; and [§]Laboratory of Cellular and Molecular Immunology, Free University of Brussels, 1050 Brussels, Belgium

¹N.G. and M.F. contributed equally to the direction of this work.

Received for publication August 31, 2010. Accepted for publication July 1, 2011.

This work was supported by Ministerio de Ciencia y Tecnología (SAF2007-61716 and SAF2005-02220); Fondo de Investigaciones Sanitarias (PS09/00538); Red Temática de Investigación en Enfermedades Cardiovasculares (RECAVA RD06/0014/1013); Red de Investigación de Centros de Enfermedades Tropicales (RICET RD06/0021/0016); European Union (HEALTH-FE-2008-22303, ChagasEpiNet); Universidad Autónoma de Madrid and Comunidad de Madrid (CC08-UAM/SAL-4440/08); Agencia Española de Cooperación Internacional para el Desarrollo cooperation with Argentina (A/025417/09); and Fundación Ramón Areces. H.C. and N.A.G. were financed by Fondo de Investigaciones Sanitarias, Instituto de salud Carlos III contracts. S.C. was a holder of a Formación de personal investigador fellowship. A.B. was funded by the Interuniversity Attraction Pole Program of the Belgian government.

Address correspondence and reprint requests to Dr. Núria Gironès, Centro de Biología Molecular Severo Ochoa, CSIC-UAM, Departamento de Bioquímica y Biología Molecular, Facultad de Ciencias, Universidad Autónoma de Madrid, Cantoblanco, 28049 Madrid, Spain. E-mail address: ngirones@cbm.uam.es

The online version of this article contains supplemental material.

Abbreviations used in this article: BCA, bicinchoninic acid; BI, PBMCs of infected mice; BNI, PBMCs of noninfected mice; CVB3, Coxsackie virus B3; dpi, days postinfection; HI, hearts of infected mice; iNOS, inducible NO synthase; L-NAME, L-N^G-nitroarginine methyl ester (hydrochloride); L-NMMA, N^G-monomethyl-L-arginine; MDSC, myeloid-derived suppressor cell; NI, noninfected mice; nor-NOHA, N^o-hydroxy-nor-L-arginine; RQ, relative quantity.

Copyright © 2011 by The American Association of Immunologists, Inc. 0022-1767/11/\$16.00

located or the pathological condition. In addition, in tumor-induced MDSCs, discrete subpopulations with distinct T cell suppressive activity have been identified (14). Therefore, a rigid classification for MDSCs is not actually available, and their definition is still a matter of debate.

Arginase I and iNOS, either separately or in combination, can inhibit T cell responses. L-Arginine is required for T cell proliferation, and the threshold of L-arginine concentration in mammalian plasma that permits fully functional T cell proliferation is 100 μM (15). Moreover, combined activity of arginase I and iNOS enzymes has been shown to be important in the suppressive activity of mouse MDSCs in tumors (16), but there also exists various evidence of the role of MDSCs, iNOS, and L-arginine depletion in infectious diseases such as chronic infections with helminths (17). In addition, in experimental infections with *T. cruzi*, the existence of an IFN- γ -induced, NO-dependent mechanism of T cell suppression has been described (5, 18).

We have previously reported the existence of a population of infiltrating myeloid cells expressing arginase I in the hearts of mice during the acute phase of Chagas disease (19). The aim of this work was to characterize the heart-infiltrating myeloid CD11b⁺ cells in acute *T. cruzi* infection. We found that the heart-infiltrating myeloid CD11b⁺ cells included granulocytic Ly6G⁺ and monocytic Ly6G⁻ subpopulations; the phenotype and function of the latter cells indicate that they are closely related to the so-called MDSCs. The monocytic myeloid cell subset, but not the granulocytic subset, expressed arginase I and iNOS activity and was able to inhibit T cell proliferation in vitro in an NO-dependent manner. Persistent arginase I expression leads to a decreased plasma L-arginine concentration during acute infection. Notably, supplementation of infected mice with L-arginine diminished parasite load. To our knowledge, this is the first report about MDSCs infiltrating the heart, in the context of myocarditis, and of plasma L-arginine depletion during acute *T. cruzi* infection, which are able to downregulate the immune response. This may have consequences in chronic cardiac Chagas disease.

Materials and Methods

Parasites and mice

Young adult (6- to 8-wk-old) BALB/c and C57BL/6 mice were purchased from Charles River Laboratories. All the infections were performed with the Y strain of *T. cruzi*. Blood trypomastigotes were routinely maintained by infecting mice and purifying them from their blood. For experiments, 2×10^5 trypomastigotes per mouse was inoculated by i.p. injection. Parasitemia was monitored by the Brener method as described (20). When indicated, mice were supplemented with 1 mg/ml L-N^G-nitroarginine methyl ester (hydrochloride) (L-NAME) or 3.75 mg/ml L-arginine in the drinking water, which was replaced every other day.

Ethics statement

This study was carried out in strict accordance with the recommendations of Spanish legislation and the European Council directive from the Convention for the Protection of Vertebrate Animals Used for Experimental and Other Scientific Purposes (21). All mice were maintained under pathogen-free conditions in the animal facility at the Centro de Biología Molecular, Universidad Autónoma de Madrid (Madrid, Spain). The animal protocol was approved by the Comité de Ética de la Investigación de la Universidad Autónoma de Madrid. Animals had free access to food and water and were handled in compliance with European norms. Mice were euthanized in a CO₂ chamber, and all efforts were made to minimize suffering.

Elicitation of organs and T, CD11b, and Ly6G magnetic cell sorting

In each experiment, 5–15 BALB/c or C57BL/6 mice were infected i.p. Mice were euthanized, at different days postinfection, in a CO₂ chamber, and hearts were aseptically removed, perfused with 10 ml PBS–heparin solution, and kept in cold HBSS. Then, hearts were pooled in a cell culture

dish, washed thoroughly with HBSS, and minced into small pieces with a sterile surgical blade. Heart pieces were then processed with a Gentle-Macs (Miltenyi Biotech) and with an enzyme mixture following the directions of the manufacturer. The cell pellet was resuspended in RPMI 1640 supplemented with 5% FBS. Blood from infected and noninfected mice was obtained by cardiac puncture and treated with heparin. Spleen cells were obtained by mechanical disruption of spleens and passed through a 40- μm cell strainer (BD Falcon). Single-cell suspension of PBMCs and spleen cells was depleted of erythrocytes by hypotonic lysis and washed with cold PBS. Peritoneal cell exudates were obtained after peritoneal cavity lavage of noninfected mice with 7 ml of a solution of sucrose (116 g/l) in PBS. CD11b⁺ cells were purified from heart, blood, spleen, and peritoneal lavage cells using CD11b microbeads (Miltenyi Biotec). T cells were isolated from spleen cells of noninfected mice with the Pan T cell kit using MACS LS columns and MACS Separators (Miltenyi Biotec) following the manufacturer's instructions. CD11b⁺ and T sorted cells were analyzed by flow cytometry and showed 95% cell purity. For Ly6G⁺ cell sorting, an anti-Ly6G microbead kit (Miltenyi Biotec) was used with the above-mentioned separating system. The Ly6G⁻ fraction of the cell suspension was 95% pure and was afterward processed for CD11b sorting and Giemsa staining.

mRNA analysis by quantitative RT-PCR

Total RNA was extracted from heart, blood, or isolated cells in TRIzol reagent (Invitrogen) as indicated by the manufacturer. For quantitative RT-PCR analysis, in indicated experiments, reverse transcription of total RNA was performed using the components of the High Capacity cDNA Archive Kit (Applied Biosystems), and amplification of different genes [*Arginase (Arg)1*, *Arg2*, *NO synthase (Nos)2*, *Tlr2*, *Tlr4*, *PG (Pstg)1*, *Ptgs2*, *Ccl2*, *Ccl3*, *Ccl5*, *Ccl17*, *Cxc2*, *Cxcl9*, *Cxcl10*, *Cxcl12*, *Il1b*, *Il4*, *Il6*, *Il10*, *Il12a*, *Il13*, *Tnf*, *Ifng*, *Tgfb*, S100 calcium binding protein (*S100a8* and *S100a9*, and ribosomal housekeeping *S18*)] was performed using the corresponding mouse TaqMan MGB probes and the TaqMan Universal PCR Master Mix (Applied Biosystems) on an ABI Prism 7900 HT instrument (Applied Biosystems). M2 gene signature expression was carried out, in indicated experiments, using Superscript II reverse transcriptase (Invitrogen) for reverse transcription and iQ SYBR Green Supermix (Bio-Rad, Hercules, CA) for quantitative RT-PCR in an iCycler (Bio-Rad) for the identified common M2 signature including *macrophage mannose receptor (Mrc1)*, *found in inflammatory zone (Fizz) 1 (Retna)*, *macrophage galactose-type C-type lectin (Mgl)2*, *Chitinase 3-like 3/4 (Ch3l3/4)*, *cadherin-1 (Cdh1)*, *plasma platelet-activating factor acetylhydrolase (Pla2g7)*, *prosaposin (Psap)*, *selenoprotein (Sepp)1*, *folate receptor (Folr)2*, and *triggering receptor expressed on myeloid cells (Trem)2* as previously described (12). All samples were run in triplicate. Quantification of gene expression by real-time PCR was calculated by the comparative threshold cycle (C_T) method following the manufacturer's instructions. All quantifications were normalized to the housekeeping gene, as indicated, to account for the variability in the initial concentration of RNA and in the conversion efficiency of the reverse transcription reaction (ΔC_T) and to values from control samples (CD11b⁺ cells from blood or peritoneal exudates, as indicated) from noninfected mice ($\Delta\Delta C_T$). The relative quantity (RQ) when using TaqMan probes was calculated as $RQ = 2^{-\Delta\Delta C_T}$. Graphs were plotted as RQ or log RQ. The fold induction for M2 gene expression analysis was normalized against the housekeeping gene *S12*.

Protein expression analyses

Protein was determined by Western blot analyses. Protein extracts were prepared in PBS containing 0.1% Triton X-100, 100 $\mu\text{g/ml}$ pepstatin, 100 $\mu\text{g/ml}$ aprotinin, and 100 $\mu\text{g/ml}$ antipain. Protein concentration was determined by the bicinchoninic acid (BCA) method (Pierce). Western blot analyses were performed as follows: 20 μg tissue extract was fractionated on SDS 10 or 15% polyacrylamide gel and transferred to a nitrocellulose membrane (Hybond-ECL; Amersham). When indicated, protein loading was visualized by Ponceau staining (Sigma). Primary Abs were diluted as follows: goat anti-mouse arginase I (V-20; Santa Cruz Biotechnology) 1:1000, S100A8 and S100A9 (R&D Systems) 1:500, purified anti-mouse iNOS (BD Transduction) 1:500, and goat anti-mouse actin (I-19; Santa Cruz Biotechnology) 1:1000. Then, the membranes were incubated with HRP-conjugated rabbit anti-goat (Sigma) 1:10,000 or goat anti-mouse (Pierce) 1:1000 Abs. Detection was carried out with Supersignal detection reagent (Pierce) and photographic film exposure.

Flow cytometry

Staining was performed in 96-well plates (Nunc). Single-cell suspensions were fixated with paraformaldehyde 1% in PBS for 1 h at 4°C. Cells were

washed with cold PBS throughout the whole staining procedure. Fc receptors on cells were blocked by incubating with purified anti-CD16/CD32 Ab (Mouse BD Fc Block; BD Pharmingen) for 15 min at 4°C. Cells were then stained with the different conjugated Abs, washed, and acquired on a FACSCanto Cytometer (Becton Dickinson). For intracellular staining, after the staining of surface molecules, cells were incubated 15 min in the presence of 0.2% saponin, washed, and incubated for 20 min with anti-CD68, washed again, and acquired as mentioned above. All data were analyzed with the FlowJo software (Tree Star).

Abs used were the following: PE-Cy7-conjugated or Alexa Fluor 647-conjugated anti-CD11b (clone M1/70; BD Pharmingen), FITC-conjugated or PE-conjugated anti-Ly6G/Ly6C (Gr-1, clone RB6-8C5; BD Pharmingen), Alexa Fluor 647-conjugated anti-Ly6C (clone AL-21; AbD Serotec), PE-conjugated anti-CD68 (FA-11; AbD Serotec), PE-conjugated anti-MHC class II (I-A/I-E, clone M5/114.15.2; eBioscience), PE-conjugated anti-F4/80 (clone BM8; AbD Serotec), PE-conjugated anti-CD11c (clone HL3; BD Pharmingen), FITC-conjugated anti-CD49b (clone DX5; eBioscience), and FITC-conjugated anti-CCR3 (clone 83101; R&D Systems). PE-conjugated Armenian hamster IgG1 (BD Pharmingen), PE-conjugated rat IgG2a (BD Pharmingen), FITC-conjugated rat IgG2a (AbD Serotec), PE-Cy7-conjugated rat IgG2b (BD Pharmingen), and FITC-conjugated rat IgM (eBioscience) Abs were used as isotypic controls.

Proliferation assays

Purified CD11b⁺ cells from hearts of infected mice and blood from noninfected mice were obtained as described earlier, counted, and resuspended in complete RPMI 1640 with 0, 100, and 1000 μ M L-arginine supplemented with 5% FBS. A total of 2×10^5 cells per well were plated in flat 96-well plates (Nunc). T cells sorted from the spleens of noninfected mice were resuspended in the same media and plated with or without CD11b⁺ purified cells isolated from hearts of infected mice or blood or spleens from noninfected mice in a 1:1 ratio. Cell cultures were stimulated with 5 μ g/ml purified anti-CD3 (BD Pharmingen) and 1 μ g/ml purified anti-CD28 Ab (BD Pharmingen), and, when indicated, 24 μ M N^G-hydroxynor-L-arginine (nor-NOHA; Calbiochem) or 2 mM N^G-monomethyl-L-arginine (L-NMMA; Calbiochem) were added. After incubation at 37°C and 5% CO₂ for 24 h, 1 μ Ci [³H]thymidine (Amersham Pharmacia Biotech) was added to each well. Cells were then harvested on a glass-fiber filter by use of a Cell Harvester (Skatron Instruments), and radioactivity was estimated in a micro β counter (Maxwell) and incorporation expressed as counts per minute.

L-Arginine determination in plasma and culture supernatants

Plasma and 1:10 diluted supernatants from cultured cells were centrifuged at 14,000 rpm to remove protein precipitates, and 5 μ l was subjected to HPLC analysis for L-arginine determination using an HPLC chromatograph coupled to a triple quadrupole mass spectrometer (Varian 1200L; Agilent Technologies).

Statistical analysis

For in vivo experiments, data are reported as means \pm SEM from triplicate determination of a representative experiment of at least two independent experiments with different experimental conditions. Results shown from in vitro experiments are representative of at least two experiments performed in triplicate. Significance was evaluated by Student *t* test with GraphPad Prism version 5.00 for Windows (GraphPad Software, San Diego CA); the Welch correction was applied when different variances were observed. All differences mentioned were significant compared with controls (**p* < 0.05, ***p* < 0.01, and ****p* < 0.001).

Results

Characterization of CD11b⁺ cells from the hearts of *T. cruzi*-infected mice

We previously described a population of myeloid cells expressing arginase I infiltrating the hearts of mice during acute *T. cruzi* infection (19). To characterize further the myeloid-infiltrating cells, CD11b⁺ populations from hearts of infected mice (HI) were isolated at the time in which arginase I heart tissue expression was maximal [14 d postinfection (dpi) and 21 dpi in C57BL/6 and BALB/c mice, respectively] (19). For comparison purposes, we used CD11b⁺ cells from peripheral blood of noninfected mice

(BNI) because hearts from the latter mice were devoid of CD11b⁺ cell infiltration. CD11b⁺ cells from the blood of infected mice (BI) were also purified and characterized. The results showed that arginase I protein expression was strongly upregulated in CD11b⁺ HI cells in comparison with CD11b⁺ BNI cells both in C57BL/6 and BALB/c infected mice (Fig. 1). Arginase I protein was also expressed in CD11b⁺ BI cells, but at lower level than that in CD11b⁺ HI cells. Arginase I protein expression was higher in BALB/c than in C57BL/6 mice in the three cell types investigated likely reflecting the fact that BALB/c mice are more prone to develop Th2 and M2 responses (22). Notably, iNOS protein expression was detected in CD11b⁺ HI cells, but not in CD11b⁺ BI and BNI cells from C57BL/6 and BALB/c mice (Fig. 1).

We analyzed the expression of several genes by quantitative RT-PCR in CD11b⁺ HI purified cells from infected BALB/c mice at 21 dpi, including: proinflammatory/M1-associated cytokines and chemokines genes required for protection against *T. cruzi* infection; anti-inflammatory/regulatory/M2-associated cytokines and chemokines that favor parasite replication; and TLRs involved in *T. cruzi* recognition. Gene expression analysis of the genes coding for arginase I (*Arg1*) and iNOS (*Nos2*) in infected BALB/c paralleled the protein expression data (Fig. 2A versus Fig. 1). The expression of *Arg2* in CD11b⁺ HI and BI cells was impaired compared with that in CD11b⁺ BNI cells. In contrast, in CD11b⁺ HI cells, gene expression of *Tlr2* in comparison with that in CD11b⁺ BNI cells was increased, whereas *Tlr4* was reduced (Fig. 2B). *Ptgs1* and *Ptgs2* genes coding for cyclooxygenase 1 and 2 enzymes and involved in the production of inflammatory mediators were downregulated and upregulated, respectively, in CD11b⁺ HI cells in comparison with that in the CD11b⁺ BNI cells (Fig. 2C). M1 chemokine genes, previously reported to be expressed in heart tissue during *T. cruzi* infection, such as *Ccl2* and *Cxcl9* (23) were found to be expressed at higher levels in CD11b⁺ HI cells with respect to CD11b⁺ BNI cells, whereas *Ccl3*, *Ccl5*, *Cxcl2*, *Cxcl10*, and *Cxcl12* showed a more discrete induced expression. The M2-associated chemokine gene *Ccl17* did not show a significant increment of expression in CD11b⁺ HI cells (Fig. 2D). CD11b⁺ HI cells also showed strong gene expression encoding for the regulatory cytokine IL-10 (*Il10*) and, at a lower level, proinflammatory cytokines such as *Il6*, *Ifng*, *Il12a*, and *Tnf*, whereas other anti-inflammatory cytokines showed downregulation (*Il4*, *Il13*, and *Tgfb1*; Fig. 2E). It should be mentioned that in general, the trend of the modulation of expression was similar in CD11b⁺ HI and BI cells of the different genes tested, with the exception of

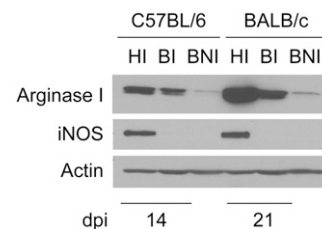


FIGURE 1. Expression of iNOS and arginase I proteins in CD11b⁺ HI cells from *T. cruzi*-infected C57BL/6 and BALB/c mice. Mice were infected i.p. with 2×10^3 blood trypomastigotes of the Y strain and sacrificed at day 14 and 21 postinfection as indicated, and infected hearts and blood from infected and noninfected mice were collected. After mechanical and enzymatic digestion of heart tissue and PBMCs purification, CD11b⁺ cells were purified with CD11b microbeads. Protein extracts were isolated; 20 μ g loaded in 10% SDS-PAGE gels and subjected to Western blot analyses using anti-arginase I or anti-iNOS Abs. Data are representative of three independent experiments.

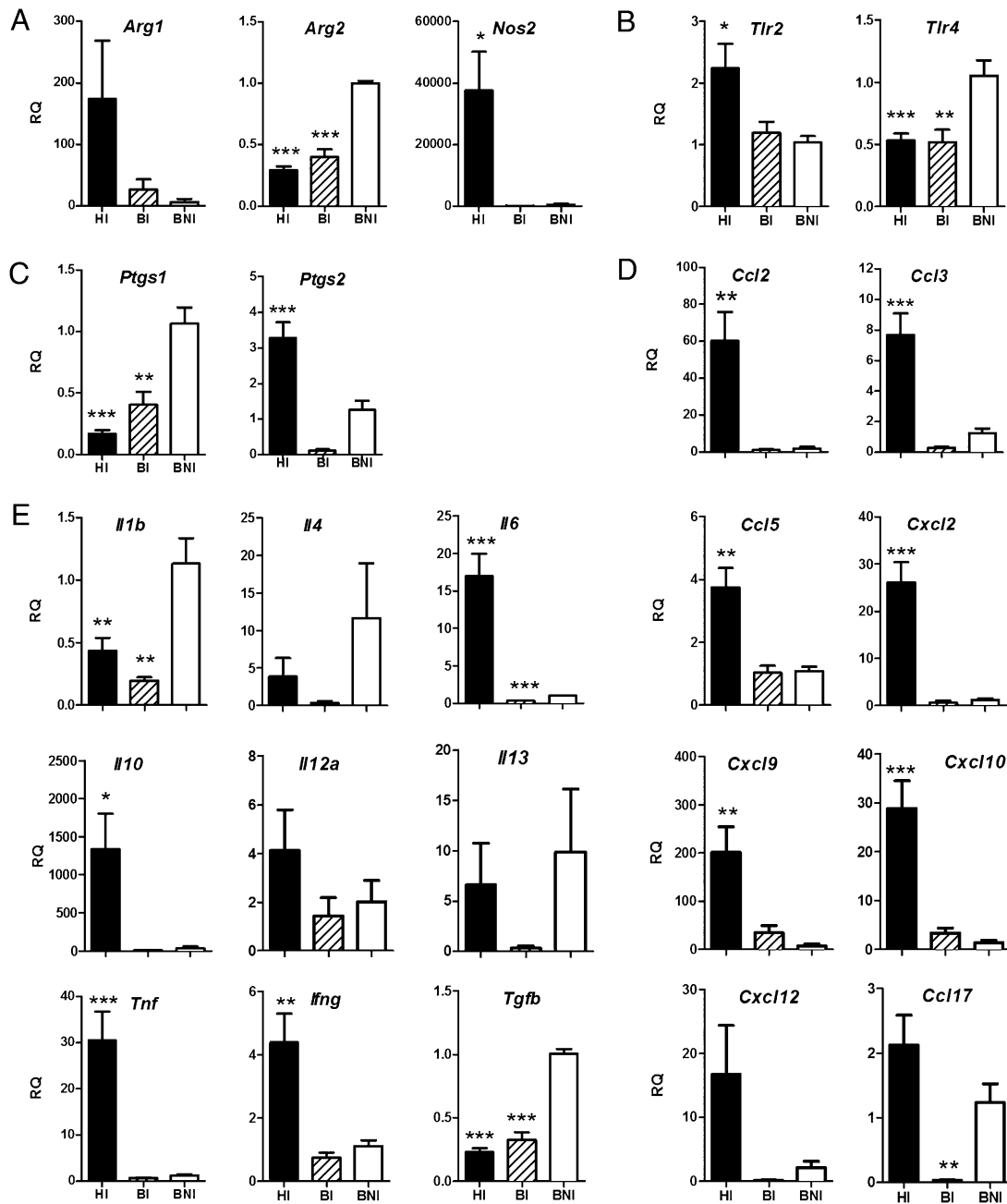


FIGURE 2. Gene expression in CD11b⁺ cells purified from hearts of *T. cruzi*-infected BALB/c mice. BALB/c mice were infected i.p. with 2×10^3 blood trypomastigotes of the Y strain. Mice were sacrificed at day 21 postinfection, and infected hearts and blood from infected and noninfected mice were elicited. After mechanical and enzymatic digestion of heart tissue and PBMCs purification, CD11b⁺ cells were purified with CD11b microbeads. HI, black bars; BI, dashed bars; BNI, white bars. mRNA was isolated from cells, and (A) *Arg1*, *Arg2*, and *Nos2*, (B) *Tlr2* and *Tlr4*, (C) *Ptgs1* and *Ptgs2*, (D) chemokines (*Ccl2*, *Ccl3*, *Ccl5*, *Cxcl2*, *Cxcl9*, *Cxcl10*, *Cxcl12*, and *Ccl17*), and (E) cytokines (*Il1b*, *Il4*, *Il6*, *Il10*, *Il12a*, *Il13*, *Tnf*, *Ifng*, and *Tgfb*) expression was analyzed by quantitative RT-PCR using TaqMan probes. Data are the mean of three independent experiments. Statistically significant differences of HI and BI with respect to BNI are shown: **p* < 0.05, ***p* < 0.01, ****p* < 0.001.

the genes coding for *Ptgs2*, *Il4*, and *Ccl17*, which were down-regulated in BI cells but upregulated in HI cells compared with that in BNI cells (Fig. 2). We also investigated gene expression of the CD11b⁺ HI isolated cells by quantitative RT-PCR of 10 markers of M2 activation previously described (12). The results showed that some M2 genes such as *Psap*, *Trem2*, *Ch3l3/4*, *Cdh1*, and *Folr2*, but not others such as *Retna*, *Sepp1*, and *Mgl2*, were significantly overexpressed in CD11b⁺ HI cells compared with that in purified CD11b⁺ of noninfected BALB/c mice (Table I). Therefore, we can conclude that heart-infiltrating CD11b⁺ cells

during *T. cruzi* infection do not show a typical M1 or M2 signature, likely reflecting the heterogeneity of the CD11b⁺ population.

Heterogeneity of the CD11b⁺ cells purified from the hearts of T. cruzi-infected mice

Next, the composition of the CD11b⁺ HI sorted population was analyzed by flow cytometry. Within purified CD11b⁺ cells, ~70% were Ly6G⁻ and 25% were Ly6G⁺ (Fig. 3A), suggesting the presence of two major subpopulations, respectively a monocytic and a granulocytic subpopulation. This was supported by the

Table I. M2 gene signature expression levels in CD11b⁺ HI as determined by real-time PCR

Gene	Fold Increase ^a
<i>Fizz (Retna)</i>	Not detected
<i>Pla2g7</i>	2.05
<i>Psap</i>	16.71 ^b
<i>Sepp1</i>	0.15
<i>Trem2</i>	5.81 ^b
<i>Mgl2</i>	0.1
<i>Ch3l3/4</i>	26,075.97 ^b
<i>Mrc1</i>	5.33 ^b
<i>Cdh1</i>	112.89 ^b
<i>Folr2</i>	6.81 ^b

^aOn day 21 postinfection, normalized with the ribosomal S12 gene and expressed relative to peritoneal exudates cells from noninfected mice. Data are shown as mean of three individual experiments.

^bFold increase >5.

observation that 1) CD11b⁺Ly6G⁻ cells expressed higher levels of Ly6C (monocytic marker), CD68 (mature macrophage marker), and MHC class II molecules compared with those of CD11b⁺Ly6G⁺ cells and 2) the CD11b⁺Ly6G⁺ cells included a higher percentage of CCR3⁺ eosinophils than that of the CD11b⁺Ly6G⁻ cells. DX5⁺ NK cells were detected only in the CD11b⁺Ly6G⁺ cell population. Finally, neither CD11b⁺Ly6G⁻ nor CD11b⁺Ly6G⁺ cell subpopulations expressed the B cell marker B220 (data not shown), the macrophage marker F4/80, or the dendritic cell marker CD11c (Fig. 3B). Together, these data show that CD11b⁺ HI cell composition is heterogeneous with mainly a monocytic and a granulocytic/NK cell fraction.

CD11b⁺ cells isolated from heart tissue of infected mice suppress T cell proliferation by an NO-dependent mechanism

In addition to arginase I and iNOS expression, suppression of T cell proliferation is the characteristic that best defines MDSCs (10, 13). Thus, we analyzed T cell proliferation upon anti-CD3/anti-CD28 Ab stimulation in the presence of CD11b⁺ HI cells using CD11b⁺ BNI cells as control. Fig. 4A shows that compared with CD11b⁺ BNI cells, CD11b⁺ HI cells were able to suppress proliferation of stimulated T cells. The addition of iNOS inhibitor L-NMMA to the cultures, but not of arginase inhibitor nor-NOHA, partially restored T cell proliferation (Fig. 4A), suggesting that CD11b⁺ HI-mediated suppression was likely mediated by an NO-dependent mechanism. However, it is known that extracellular L-arginine concentrations below 100 μM impair fully functional T cell proliferation (15). Therefore, we studied T cell proliferation in medium containing different concentrations of L-arginine (0, 100, and 1000 μM) in the presence and absence of CD11b⁺ cells from spleens of noninfected mice (NI), (Fig. 4B and 4C, respectively). The results showed that T cell proliferation was dependent on L-arginine concentration, and addition of CD11b⁺ cells to the culture significantly incremented T cell proliferation with respect to T cells alone. Therefore, to test the contribution of arginase I to T cell suppression by L-arginine depletion, we lowered L-arginine concentration in the culture medium to 100 μM and compared the effect of CD11b⁺ HI cells (Fig. 4D) with cultures of T cells alone. The results showed that when T cells were cultured with CD11b⁺ HI cells, there was a strong suppressive effect on T cell proliferation. Addition of iNOS and arginase I inhibitors to activated T cells cultured alone did not significantly affect their proliferation. However, similar to cultures performed in >1 mM L-arginine (Fig. 4A), there was a partial recovery of T cell proliferation in the presence of L-NMMA, but not in the presence of

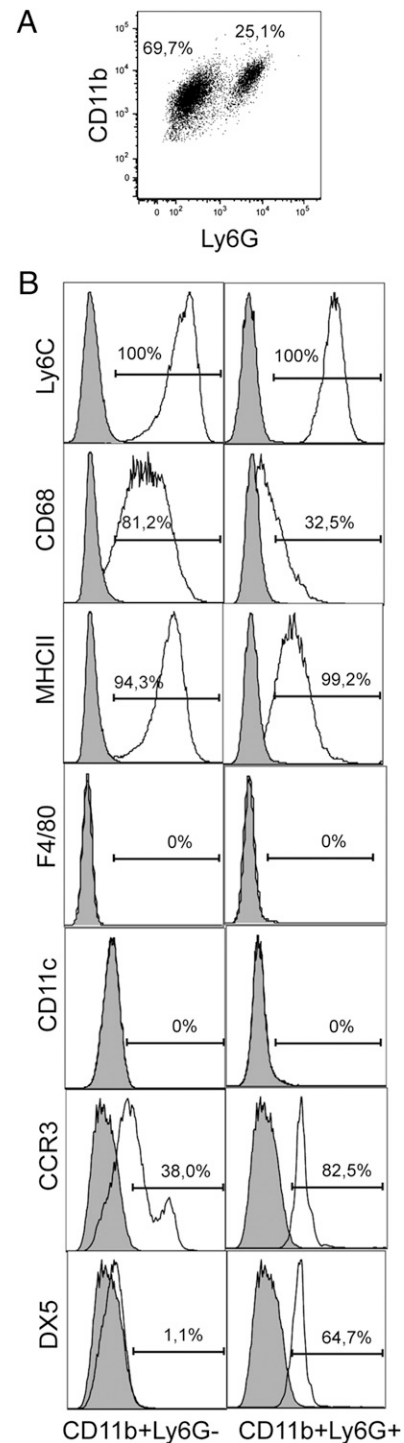


FIGURE 3. Flow cytometry analysis of CD11b⁺ cells purified from hearts of *T. cruzi*-infected BALB/c mice. Mice were infected i.p. with 2×10^3 blood trypomastigotes of the Y strain. Mice were sacrificed at day 21 postinfection, and infected hearts were elicited. After mechanical and enzymatic digestion of heart tissue, CD11b⁺ cells were purified with CD11b microbeads. Cells were stained with anti-CD11b-PE-Cy7 or anti-CD11b-Alexa Fluor 647, anti-Ly6G/Ly6C(Gr-1)-FITC or anti-Ly6G/Ly6C(Gr-1)-PE, anti-Ly6C-Alexa Fluor 647, anti-CD68-PE, anti-MHCII-PE, anti-F4/80-PE, anti-CD11c-PE, anti-CCR3-FITC, and anti-CD49b(DX5)-FITC Abs and analyzed in FACSCanto. Gray histograms represent isotypic Ab labeling and white histograms specific staining as indicated. **A**, Double staining with Ly6G/Ly6C and CD11b Abs. **B**, Staining of CD11b⁺Ly6G⁻ and CD11b⁺Ly6G⁺ gated populations with Ly6C, CD68, F4/80, MHCII, CD11c, CCR3, and DX5 Abs. Data are representative of at least three independent experiments. MHCII, MHC class II.

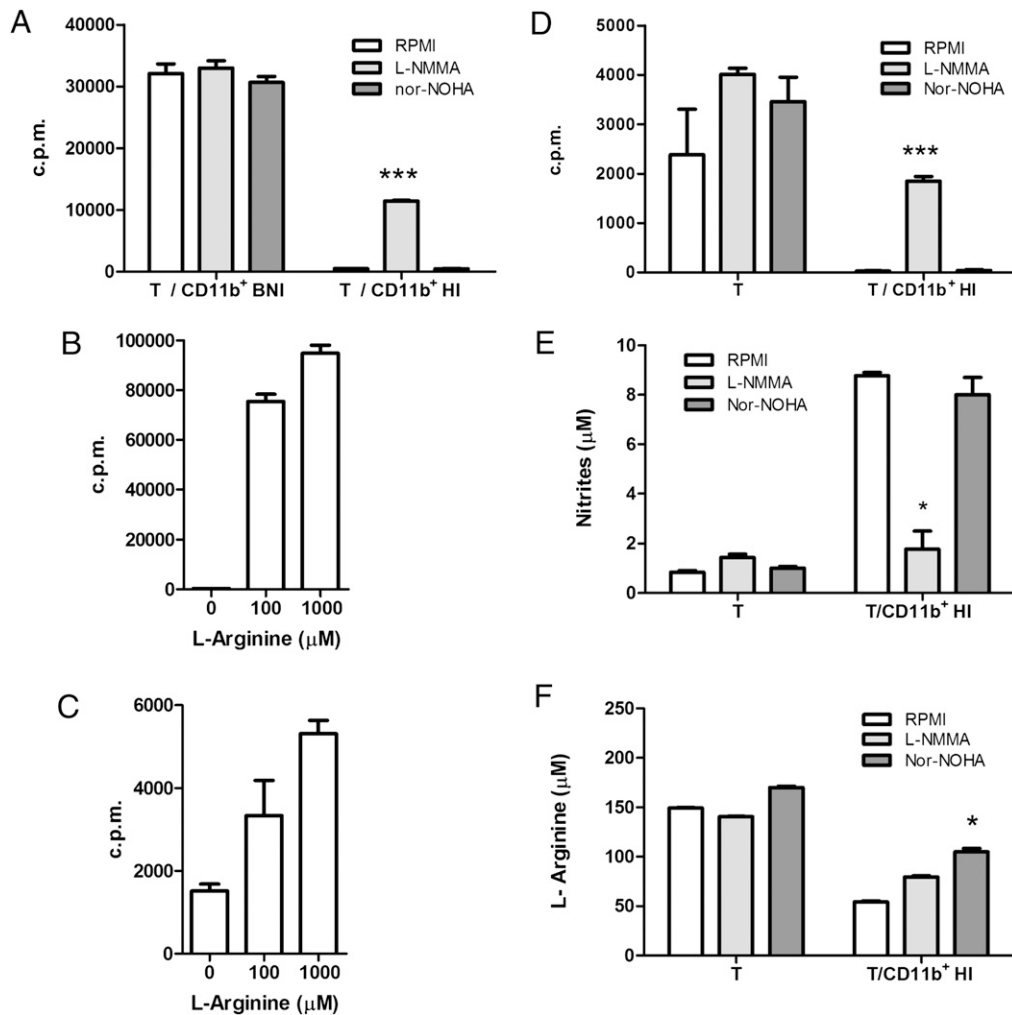


FIGURE 4. Suppression of T cell proliferation in the presence of CD11b⁺ HI cells from *T. cruzi*-infected BALB/c mice. Mice were infected i.p. with 2×10^3 blood trypomastigotes of the Y strain. Mice were sacrificed at day 21 postinfection, and infected hearts were collected. After mechanical and enzymatic digestion of infected heart tissue (HI) and isolation of blood from noninfected mice (BNI), CD11b⁺ cells were purified with CD11b microbeads. T cells were isolated from spleens of noninfected mice (T) with the Pan T cell kit, and the proliferation assays were set up as follows. *A*, T cells were activated with anti-CD3 and anti-CD28 Abs and cultured with RPMI 1640 with 1 mM L-arginine in the presence of CD11b⁺ BNI or CD11b⁺ HI cells and the presence or absence of iNOS (L-NMMA) and arginase I (nor-NOHA) inhibitors. *B* and *C*, Activated T cells were cultured with CD11b⁺ cells isolated from noninfected mice (*B*) or alone (*C*) in presence of indicated concentrations of L-arginine. *D*, Activated T cells were cultured with 100 μM L-arginine in the presence or absence of CD11b⁺ HI cells and inhibitors (L-NMMA and nor-NOHA). *E*, Concentration of nitrites (NO₂Na) was measured in the supernatants of the cultures from *D* with the Griess reagent. *F*, Concentration of extracellular L-arginine was measured in the supernatants of the cultures from *D* using an HPLC chromatograph coupled to a mass detector. Data are representative of at least two independent experiments. Statistically significant differences with respect to cultures with RPMI medium of each condition are shown: **p* < 0.05, ****p* < 0.001.

nor-NOHA (Fig. 4*B*), suggesting that, *in vitro*, even at reduced L-arginine concentration, suppression of proliferation is mostly mediated by NO. In agreement, the concentration of nitrite increased significantly in the culture supernatants in the presence of CD11b⁺ cells, and this was inhibited upon addition of L-NMMA (Fig. 4*E*). Finally, Fig. 4*F* shows that the concentration of L-arginine was still above the threshold that allows basal T cell proliferation (~100 μM). Additional L-arginine present in the supernatants (150 μM) could come from the FBS added to the RPMI 1640 medium and from intracellular pools. Notably, CD11b⁺ HI cells caused a drastic reduction of L-arginine concentration in medium when these cells were cocultured with activated T cells. This was significantly recovered in the presence of arginase inhibitor, indicating that arginase is active in CD11b⁺ HI cells. Taken together, the above results indicate that CD11b⁺ HI cell *in vitro* T cell immunosuppression is mediated by iNOS.

Purified CD11b⁺Ly6G⁻ monocytic cells isolated from heart tissue of infected mice express iNOS and arginase I and suppress, in vitro, T cell proliferation by an NO-dependent mechanism

To characterize in more detail the cells expressing arginase I and iNOS, Ly6G⁺, CD11b⁺Ly6G⁻, and CD11b⁻Ly6G⁻ cells isolated from hearts of *T. cruzi*-infected mice were cultured with activated T cells. Fig. 5*A* and Table II show that, after magnetic sorting, ~35% of the cells were Ly6G⁺ and 65% were Ly6G⁻, in agreement with flow cytometry analysis (Fig. 3). We recovered an average of 1.57×10^5 ($\pm 0.30 \times 10^5$) Ly6G⁺ cells and 2.96×10^5 ($\pm 0.57 \times 10^5$) Ly6G⁻ per heart of BALB/c infected mice. Microscopic examination of 20 different fields of Giemsa-stained cells showed that the phenotype of the Ly6G⁻ cells was predominantly monocytic, whereas Ly6G⁺ cells were ~70% granulocytic and 30% nongranulocytic (Table II and Supplemental

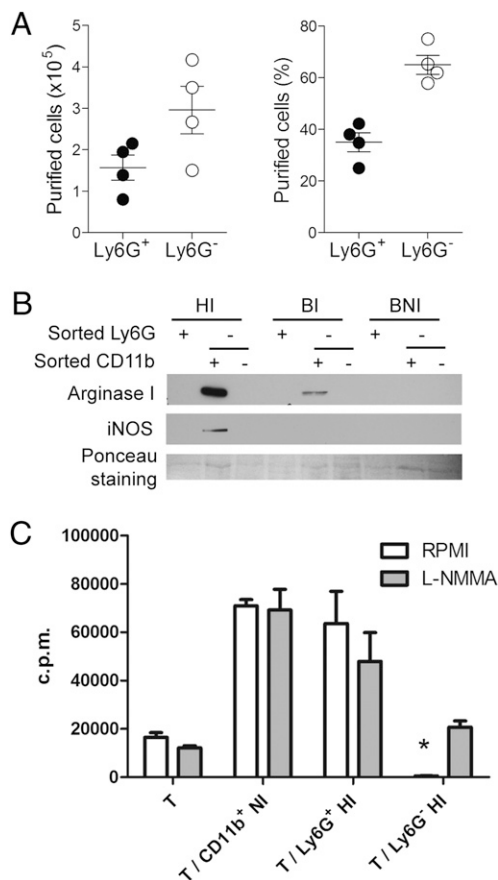


FIGURE 5. Expression of iNOS and arginase I in CD11b⁺ Ly6G⁻ HI cells suppresses T cell proliferation. BALB/c mice were infected i.p. with 2×10^3 blood trypomastigotes of the Y strain. Mice were sacrificed at day 21 postinfection, and infected hearts and blood were elicited. Hearts were mechanically and enzymatically digested and PBMCs purified from blood of infected and noninfected mice. Cells were purified with Ly6G microbeads, and the resulting Ly6G⁻ cells were subsequently purified with CD11b microbeads. **A**, Average number and percentage of purified cells per heart of *T. cruzi*-infected BALB/c mice. **B**, Protein content was quantified by BCA method and analyzed; 20 μ g loaded in 10% SDS-PAGE gels and subjected to Western blot with Abs against arginase I and iNOS. A representative Ponceau-stained band is shown as loading control. **C**, Proliferative assay of anti-CD3- and anti-CD28-stimulated T cells in the absence and presence of purified CD11b⁺ cells isolated from noninfected mice (CD11b⁺ NI cells), Ly6G⁺ HI cells, and Ly6G⁻ HI cells. Data are representative of at least two independent experiments. The statistically significant difference with respect to cultures of T cells alone and in the presence of CD11b⁺ cells from noninfected mice is shown: * $p < 0.05$.

Fig. 1). CD11b⁺Ly6G⁻ cells, but not Ly6G⁺ cells, expressed arginase I and iNOS by Western blot (Fig. 5B). We also detected arginase I expression in CD11b⁺Ly6G⁻ cells isolated from the blood of infected mice but not from noninfected mice (Fig. 5B), in agreement with previous observations in PBMC lysates (19). CD11b⁺Ly6G⁻ cells, but not Ly6G⁺ cells, from hearts of infected

Table II. Phenotype of magnetically sorted cells isolated from hearts of mice at 21 dpi according to Giemsa staining

Cell Type	Microscopic Examination % (20 Fields)
CD11b ⁺ Ly6G ⁺	70 granulocytic 30 nongranulocytic
CD11b ⁺ Ly6G ⁻	98 monocytic 2 nonmonocytic

mice suppressed anti-CD3/anti-CD28-stimulated T cell proliferation in comparison with T cells alone and T cells cultured with CD11b⁺ NI (Fig. 5C). Suppression was partially reverted in the presence of L-NMMA, indicating that it is mediated by NO. These results strongly support that CD11b⁺Ly6G⁻ are MDSCs.

Ly6G⁺ granulocytic cells isolated from heart tissue of infected mice express S100A8 and S100A9

MDSC recruitment into several tissues has been shown to be dependent on S100A8 and S100A9 proteins (24). Coinciding with the presence of monocytic MDSCs, our results showed that *S100a8* and *S100a9* gene and corresponding protein expression (Fig. 6A and 6B, respectively) were detected in heart tissue in the acute phase of *T. cruzi* infection in BALB/c mice, showing highest expression at 21 dpi coincident with previously described maximum arginase I and iNOS expression (19). We also detected expression of *S100a8* and *S100a9* gene and protein in C57BL/6 infected mice (Supplemental Fig. 2), although lower than that in BALB/c mice, correlating with the different kinetics of arginase I expression in heart tissue of this strain of mice infected with *T. cruzi* (19). In agreement with previous observations, the expression of another important chemokine involved in monocyte heart recruitment in *T. cruzi* infection, CCL2 (25), showed itself to be overexpressed in CD11b⁺ HI cells with respect to control cells (Fig. 2D) following similar kinetics as S100A8 and S100A9 in heart tissue of both BALB/c and C57BL/6 mice (Supplemental Fig. 3).

We next investigated the cellular origin of S100A8 and S100A9 in the heart infiltrate of *T. cruzi* infected mice. We found that S100A8 and S100A9 proteins were expressed in Ly6G⁺, which did not express iNOS and arginase I, but not in CD11b⁺Ly6G⁻ cells, which do express iNOS and arginase I (Figs. 4 and 6C). Therefore, S100A8 and S100A9 proteins expressed by granulocytic cells might be implicated in the recruitment and/or differentiation of heart-infiltrated, arginase I/iNOS-expressing MDSCs in *T. cruzi*-infected mice.

T. cruzi infection in mice causes plasma L-arginine depletion

Arginase I expression in MDSCs during *T. cruzi* infection can decrease L-arginine availability. Thus, we studied whether circulating L-arginine levels were affected in infected mice. In C57BL/6 mice, there was a substantial decrease in plasma L-arginine concentration (<50 μ M) at 14 dpi, and in BALB/c mice the reduction was observed for longer periods (at 14 and 21 dpi) (Fig. 7A, 7B). These results correlated with our previous kinetics of arginase I expression in the hearts of both C57BL/6 and BALB/c mice (19) and indicated that during in vivo infection, arginase I-expressing cells in heart tissue and/or in peripheral blood could cause plasma L-arginine depletion that can account for suppression of T cell proliferation observed in the acute phase.

To evaluate the relevance of MDSCs in hearts of *T. cruzi*-infected mice, we treated mice with the iNOS inhibitor L-NAME. The inhibition of iNOS resulted in a dramatic increase in parasitemia, mortality, and parasite load in heart tissue with respect to untreated mice (Supplemental Fig. 4). This result confirms the in vivo relevance of iNOS and, by extension, NO-producing MDSCs in *T. cruzi* infection. Of greater interest, L-arginine supplementation reduced parasite burden in heart tissue (Fig. 7C), indicating that restoration of L-arginine levels is beneficial for the host.

Discussion

The understanding of the pathogenesis of myocarditis induced by *T. cruzi* is crucial to develop therapeutic strategies aiming to ameliorate the inflammation that leads to heart dysfunction. In this

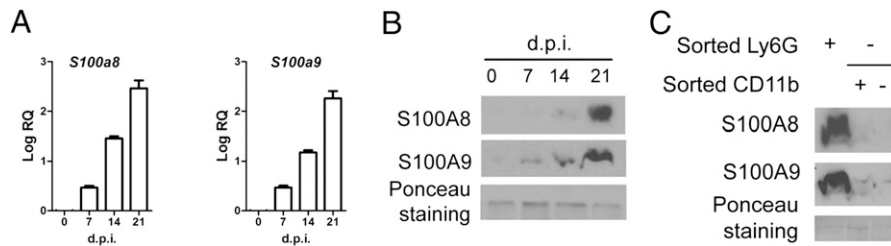


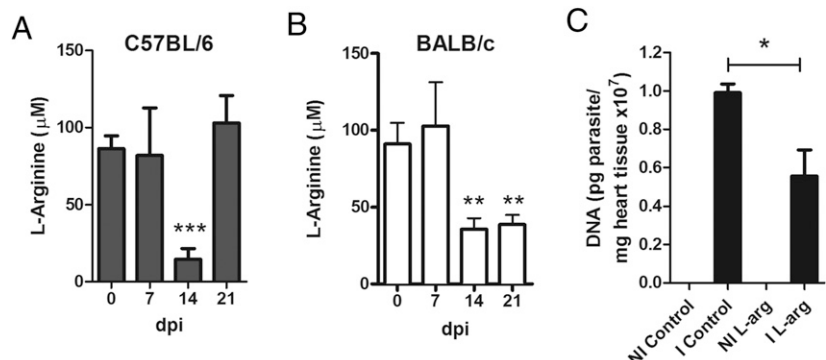
FIGURE 6. S100A8/S100A9 expression in hearts from *T. cruzi*-infected BALB/c mice and in hearts isolated cells after Ly6G and CD11b magnetic sorting. Groups of 5–15 BALB/c mice were infected i.p. with 2×10^3 blood trypomastigotes of the Y strain. Mice were sacrificed at 0, 7, 14, and 21 dpi. *A*, mRNA was extracted from hearts, and *S100a8* and *S100a9* expression was analyzed by quantitative RT-PCR. *B*, Protein extracts were isolated from heart tissue from BALB/c mice at different days postinfection; 20 μ g loaded in 15% SDS-PAGE gels and subjected to Western blot analysis with anti S100A8 and S100A9 Abs. A representative Ponceau-stained band is shown as loading control. Data are representative of at least two independent experiments. *C*, Hearts were mechanically and enzymatically digested. Cells were purified with Ly6G⁺ microbeads, and the resulting Ly6G⁺ cells were subsequently purified with CD11b microbeads. Protein content was quantified by BCA method; 20 μ g loaded in 15% SDS-PAGE gels and subjected to Western blot with Abs against S100A8 and S100A9. A representative Ponceau-stained band is shown as loading control. Data are representative of at least two independent experiments.

regard, the mouse model of *T. cruzi* infection recapitulates many of the functional and pathological alterations of the human disease. Thus, in the myocardium of acutely infected mice, there is an inflammatory reaction characterized by lymphoid and myeloid cell infiltration and expression of inflammatory mediators thought to be responsible for the pathogenesis (19). To date, most of the research has focused on the characterization of the infiltrating T lymphocytes in the myocarditis associated with *T. cruzi* infection whereas very little is known about myeloid cells present in this heart inflammatory infiltrate. Our previous results showed that myeloid cells infiltrating the heart, and to a minor extent PBMCs from *T. cruzi*-infected mice, expressed arginase I (19). In this study, we have purified those cells and analyzed their gene expression, phenotype, and function.

The myeloid CD11b⁺ population in the hearts of mice acutely infected with *T. cruzi* expresses markers of M1 and M2 subsets and is composed of two main subpopulations: immature monocytic Ly6G[−] and granulocytic Ly6G⁺. The monocytic Ly6G[−] cells, but not the granulocytic Ly6G⁺ cells, express iNOS and arginase I and are able to suppress T cell proliferation. The granulocytic Ly6G⁺ cells, but not monocytic Ly6G[−] cells, express S100A8 and S100A9 proteins. According to marker expression and especially suppressive function, our results indicate that monocytic Ly6G[−] cells are indeed MDSCs. Recruitment of MDSCs to the heart could be potentiated by granulocytic Ly6G⁺ cells through S100A8 and S100A9 protein expression. T cell suppression in vitro by those CD11b⁺Ly6G[−] cells is mostly mediated by NO, and the in vivo high level of expression of arginase I by MDSCs produces systemic depletion of L-arginine that may contribute to systemic immunosuppression in the acute phase of infection.

We found that isolated CD11b⁺ cells from the hearts of infected mice expressed both arginase I and iNOS but not arginase II. In addition, gene expression of several type 1 chemokines and cytokines was found to be selectively upregulated by CD11b⁺ HI cells. Notably, the regulatory cytokine *Il10* was also highly induced, as well as markers of M2 populations. We focused our studies in the BALB/c model, which presented higher infiltration of those cells; however, similar qualitative results were obtained in the C57BL/6 model (data not shown). The expression of M1 and M2 genes could be the result of heterogeneity of the CD11b⁺ isolated population. Nonetheless, it is accepted that coexpression of M1/M2 genes is characteristic of MDSCs (26). Moreover, a striking similar profiling of M1/M2 genes (*Il10*, *Ccl2*, and *Ccl5*, IFN-inducible chemokines *Cxcl9* and *Cxcl10*) has been described in MDSCs infiltrating tumors (27, 28). Giemsa staining of the isolated CD11b⁺Ly6G[−] HI cells revealed a monocytic phenotype. Therefore, the monocytic CD11b⁺Ly6G[−] isolated subpopulation expressing both iNOS and arginase I could be considered as bona fide MDSCs accumulating in the hearts of *T. cruzi*-infected mice. The Ly6G⁺ sorted population was more heterogeneous and showed a predominant granulocytic phenotype that was devoid of iNOS and arginase I expression. In a different model, the existence of a Ly6C⁺ granulocytic population has been described in the injured myocardium, which is recruited via CCR2 and thought to digest damaged tissue (29). In addition, CD11b⁺Gr-1⁺F4/80⁺ populations that presented mixed M2/MDSCs phenotype have been described infiltrating the heart during Coxsackie virus B3 (CVB3) viral myocarditis (9). Neither iNOS expression nor suppressor activity had been reported in the injured heart or in CVB3 myocarditis. It is worth mentioning that CD11b⁺ HI cells were F4/80[−] but CD68⁺, being both mature macrophage markers. Our

FIGURE 7. Plasma L-arginine depletion in mice infected with *T. cruzi*. BALB/c and C57BL/6 mice were infected i.p. with 2×10^3 blood trypomastigotes of the Y strain. Plasma was isolated at indicated days postinfection and L-arginine concentration determined. *A*, Values for C57BL/6 mice. *B*, Values for BALB/c mice. *C*, *T. cruzi* parasite load determined by quantitative PCR in mice with or without dietary L-arginine supplement. Data are representative of at least two independent experiments. Statistically significant difference with respect to noninfected mice (*A*, *B*) and untreated infected mice (*C*) is shown: * $p < 0.05$, ** $p < 0.01$, *** $p < 0.001$.



results indicate that *T. cruzi* infection induces the recruitment of a particular phenotype of cells different from the ones described in CVB3 myocarditis.

It is known that MDSCs express arginase I that can cause suppression of T cell proliferation by extracellular L-arginine depletion. We observed that during acute *T. cruzi* infection, there is plasma L-arginine depletion at day 14 postinfection in less susceptible C57BL/6 mice and at days 14 and 21 postinfection in more susceptible BALB/c mice. These results suggest that fast recovery from L-arginine plasma depletion in C57BL/6 mice is linked to their low susceptibility to infection. In addition, L-arginine plasma depletion nicely correlated with the kinetics of arginase I expression in isolated blood and heart CD11b⁺ cells (19) and with systemic immunosuppression (5). The mechanism of T cell suppression in vitro in *T. cruzi*-infected mice by CD11b⁺ Ly6G⁻ cells is mediated by NO, and in vivo systemic depletion of L-arginine, likely mediated by high level of expression of arginase I by those cells, may contribute to systemic immunosuppression in the acute phase of infection. Thus, according to markers, phenotype, and suppressive function, these cells are in fact bona fide MDSCs.

CD11b⁺ BI cells did not express iNOS compared with CD11b⁺ HI cells. Thus, induction of arginase I and iNOS in CD11b⁺ cells could occur after their recruitment from periphery to heart tissue, similar to what happens in tumor infiltration by myeloid cells (10, 28). In this regard, we found that only the Ly6G⁺ cells isolated from heart tissue of infected mice expressed S100A8 and S100A9 proteins. Those molecules have been described to regulate the accumulation of MDSCs (24). Thus, a plausible explanation is that Ly6G⁺ infiltrated in heart tissue could be triggering recruitment of Ly6G⁻ cells through expression of S100A8 and S100A9 proteins, which also prevent further differentiation of MDSCs to macrophages and dendritic cells. Nonetheless, we cannot discard the involvement of other chemokines as CCL2 in this recruitment. In contrast, it could be possible that blood cells expressing arginase I (but no iNOS) are M2 macrophages, a possibility that has not been addressed in this study. Alternatively, MDSCs in heart may result from expansion of resident tissue macrophages, but this is unlikely, as they do not express the mature macrophage marker F4/80. Also, the spleen has been described to function as a source of monocytes that have further ability to infiltrate the heart (30), therefore it could be that CD11b⁺ HI cells are originated and mobilized from the spleen. In this regard, we have found that spleens of *T. cruzi*-infected animals in the same days postinfection contain a CD11b⁺Gr1⁺ population that inhibits T cell proliferation via NO (5).

The goal of immune regulation is to avoid excessive production of immune mediators that could be detrimental to the host and even cause its death, as it seems to be in *T. cruzi* myocarditis (3). Thus, CD11b⁺ HI MDSCs may regulate the excessive T cell-dependent inflammation in the heart at the onset of infection, which could much later determine the severity of cardiomyopathy. Among the genes expressed by CD11b⁺ HI cells are the chemokines *Ccl2*, *Ccl5*, *Cxcl9*, and *Cxcl10* that were previously shown to be expressed in the hearts of *T. cruzi*-infected mice during the acute phase, and they play a protective role in *T. cruzi* infection but not in association with the heart inflammatory phenotype (23, 25). This indirectly would suggest a protective role of CD11b⁺ HI cells in *T. cruzi*-induced myocarditis. On the contrary, in susceptible mice, expression of iNOS and arginase I by MDSCs is higher and more prolonged in time than in nonsusceptible C57BL/6 mice, suggesting an association between MDSCs, iNOS/arginase I expression, and higher parasite burden followed by worst outcome of the disease.

A formal demonstration of the exact role of MDSCs in *T. cruzi* infection is difficult because there are no conclusive markers of those cells to allow their selective elimination in infected animals. To evaluate the relevance of MDSCs, we followed an alternative approach: we inhibited iNOS with L-NAME treatment of infected mice resulting in a dramatic increase in parasitemia, mortality, and parasite load in heart tissue with respect to untreated mice, showing that iNOS, and by extension NO-producing MDSCs, are necessary to control the *T. cruzi* infection (31–34). In addition, L-arginine supplementation reduced parasite burden in heart tissue, indicating that restoration of L-arginine levels is beneficial for the host. Because L-arginine is one of the rate-limiting factors in NO production (35), it is possible that L-arginine supplementation increases NO production in infected mice, which would end in a more efficient control of the infection. Therefore, L-arginine supplementation can have two different effects: 1) it could fuel iNOS-derived NO production, thus reducing parasite replication that is evidenced by a reduction in heart parasite load; 2) it can revert immunosuppression, thus allowing a more efficient control of infection by the immune system. Moreover, there is a strong correlation between the appearance of those cells and severity of the disease. More importantly, antagonizing or preventing the effect of arginase I and iNOS, enzymes that best define their function, modulates parasite load in heart tissue and mortality. Our results support the hypothesis that iNOS- and arginase I-expressing MDSCs are beneficial in *T. cruzi* infection when L-arginine is available but detrimental for the host when they cause persistent L-arginine depletion.

In summary, we describe in this study for the first time to our knowledge that monocytic MDSCs that express iNOS and arginase I are present in heart tissue in the acute phase of *T. cruzi* infection, where they have the potential to suppress T lymphocytes present in the infiltrate. This is the first description of MDSCs found infiltrating the heart during *T. cruzi* infection and, to our knowledge, in the context of cardiac inflammation. The presence of MDSCs correlates with depletion of L-arginine from plasma that can have a systemic suppressor effect on T cell function extending to other inflamed organs and tissues. MDSC iNOS activity may be required for efficient control of parasite load in the heart that leads to survival of infected mice, but iNOS in combination with arginase I also could be detrimental for the host when iNOS/arginase I expression is persistent through the acute phase of infection causing plasma L-arginine depletion. Cardiac and systemic effects of MDSCs are transient, and the outcome of disease may depend as well on components of the innate, adaptive, and regulatory immune responses.

Acknowledgments

We thank Beatriz Barrocal and Ella Omasta for animal care and Maria A. Chorro, Carlos Chillón, Ricardo Ramos, and Rosa Sedano for technical assistance. We also thank Kivash Movahedi and Tom Bosschaerts for discussion of the data.

Disclosures

The authors have no financial conflicts of interest.

References

1. WHO. 2002. *World Health Report*. WHO, Geneva, Switzerland.
2. Gironès, N., and M. Fresno. 2003. Etiology of Chagas disease myocarditis: autoimmunity, parasite persistence, or both? *Trends Parasitol.* 19: 19–22.
3. Marin-Neto, J. A., E. Cunha-Neto, B. C. Maciel, and M. V. Simões. 2007. Pathogenesis of chronic Chagas heart disease. *Circulation* 115: 1109–1123.
4. Muñoz-Fernández, M. A., M. A. Fernández, and M. Fresno. 1992. Synergism between tumor necrosis factor- α and interferon- γ on macrophage activation for the killing of intracellular *Trypanosoma cruzi* through a nitric oxide-dependent mechanism. *Eur. J. Immunol.* 22: 301–307.

5. Goñi, O., P. Alcaide, and M. Fresno. 2002. Immunosuppression during acute *Trypanosoma cruzi* infection: involvement of Ly6G (Gr1(+))CD11b(+) immature myeloid suppressor cells. *Int. Immunol.* 14: 1125–1134.
6. Gomes, J. A., L. M. Bahia-Oliveira, M. O. Rocha, O. A. Martins-Filho, G. Gazzinelli, and R. Correa-Oliveira. 2003. Evidence that development of severe cardiomyopathy in human Chagas' disease is due to a Th1-specific immune response. *Infect. Immun.* 71: 1185–1193.
7. Bergeron, M., and M. Olivier. 2006. *Trypanosoma cruzi*-mediated IFN- γ -inducible nitric oxide output in macrophages is regulated by iNOS mRNA stability. *J. Immunol.* 177: 6271–6280.
8. Stempin, C. C., T. B. Tanos, O. A. Coso, and F. M. Cerbán. 2004. Arginase induction promotes *Trypanosoma cruzi* intracellular replication in Cruzipain-treated J774 cells through the activation of multiple signaling pathways. *Eur. J. Immunol.* 34: 200–209.
9. Fairweather, D., and D. Cihakova. 2009. Alternatively activated macrophages in infection and autoimmunity. *J. Autoimmun.* 33: 222–230.
10. Gabrilovich, D. I., and S. Nagaraj. 2009. Myeloid-derived suppressor cells as regulators of the immune system. *Nat. Rev. Immunol.* 9: 162–174.
11. Vincendeau, P., A. P. Gobert, S. Daulouède, D. Moynet, and M. D. Mossalayi. 2003. Arginases in parasitic diseases. *Trends Parasitol.* 19: 9–12.
12. Ghassabeh, G. H., P. De Baetselier, L. Brys, W. Noël, J. A. Van Genderachter, S. Meerschaut, A. Beschin, F. Brombacher, and G. Raes. 2006. Identification of a common gene signature for type II cytokine-associated myeloid cells elicited in vivo in different pathologic conditions. *Nat. Rev. Immunol.* 108: 575–583.
13. Marigo, I., L. Dolcetti, P. Serafini, P. Zanovello, and V. Bronte. 2008. Tumor-induced tolerance and immune suppression by myeloid derived suppressor cells. *Immunol. Rev.* 222: 162–179.
14. Movahedi, K., M. Guillemins, J. Van den Bossche, R. Van den Bergh, C. Gysemans, A. Beschin, P. De Baetselier, and J. A. Van Genderachter. 2008. Identification of discrete tumor-induced myeloid-derived suppressor cell subpopulations with distinct T cell-suppressive activity. *Blood* 111: 4233–4244.
15. Choi, B. S., I. C. Martinez-Falero, C. Corset, M. Munder, M. Modollell, I. Müller, and P. Kropf. 2009. Differential impact of L-arginine deprivation on the activation and effector functions of T cells and macrophages. *J. Leukoc. Biol.* 85: 268–277.
16. Bronte, V., P. Serafini, A. Mazzoni, D. M. Segal, and P. Zanovello. 2003. L-arginine metabolism in myeloid cells controls T-lymphocyte functions. *Trends Immunol.* 24: 302–306.
17. Brys, L., A. Beschin, G. Raes, G. H. Ghassabeh, W. Noël, J. Brandt, F. Brombacher, and P. De Baetselier. 2005. Reactive oxygen species and 12/15-lipoxygenase contribute to the antiproliferative capacity of alternatively activated myeloid cells elicited during helminth infection. *J. Immunol.* 174: 6095–6104.
18. Abrahamsohn, I. A., and R. L. Coffman. 1995. Cytokine and nitric oxide regulation of the immunosuppression in *Trypanosoma cruzi* infection. *J. Immunol.* 155: 3955–3963.
19. Cuervo, H., M. A. Pineda, M. P. Aoki, S. Gea, M. Fresno, and N. Gironès. 2008. Inducible nitric oxide synthase and arginase expression in heart tissue during acute *Trypanosoma cruzi* infection in mice: arginase I is expressed in infiltrating CD68+ macrophages. *J. Infect. Dis.* 197: 1772–1782.
20. Brener, Z. 1962. Therapeutic activity and criterion of cure on mice experimentally infected with *Trypanosoma cruzi*. *Rev. Inst. Med. Trop. Sao Paulo* 4: 389–396.
21. European Council. 1986 (March 18). *Council Directive from the Convention for the Protection of Vertebrate Animals Used for Experimental and Other Scientific Purposes*. European Council, Strasbourg, France.
22. Mills, C. D., K. Kincaid, J. M. Alt, M. J. Heilman, and A. M. Hill. 2000. M-1/M-2 macrophages and the Th1/Th2 paradigm. *J. Immunol.* 164: 6166–6173.
23. Hardison, J. L., R. A. Wrightsman, P. M. Carpenter, T. E. Lane, and J. E. Manning. 2006. The chemokines CXCL9 and CXCL10 promote a protective immune response but do not contribute to cardiac inflammation following infection with *Trypanosoma cruzi*. *Infect. Immun.* 74: 125–134.
24. Sinha, P., C. Okoro, D. Foell, H. H. Freeze, S. Ostrand-Rosenberg, and G. Srikrishna. 2008. Proinflammatory S100 proteins regulate the accumulation of myeloid-derived suppressor cells. *J. Immunol.* 181: 4666–4675.
25. Paiva, C. N., R. T. Figueiredo, K. Kroll-Palhares, A. A. Silva, J. C. Silvério, D. Gibaldi, Ados, S. Pyrrho, C. F. Benjamim, J. Lannes-Vieira, and M. T. Bozza. 2009. CCL2/MCP-1 controls parasite burden, cell infiltration, and mononuclear activation during acute *Trypanosoma cruzi* infection. *J. Leukoc. Biol.* 86: 1239–1246.
26. Umemura, N., M. Saio, T. Suwa, Y. Kitoh, J. Bai, K. Nonaka, G. F. Ouyang, M. Okada, M. Balazs, R. Adany, et al. 2008. Tumor-infiltrating myeloid-derived suppressor cells are pleiotropic-inflamed monocytes/macrophages that bear M1- and M2-type characteristics. *J. Leukoc. Biol.* 83: 1136–1144.
27. Biswas, S. K., L. Gangi, S. Paul, T. Schioppa, A. Saccani, M. Sironi, B. Bottazzi, A. Doni, B. Vincenzi, F. Pasqualini, et al. 2006. A distinct and unique transcriptional program expressed by tumor-associated macrophages (defective NF- κ B and enhanced IRF-3/STAT1 activation). *Blood* 107: 2112–2122.
28. Bronte, V., and P. Zanovello. 2005. Regulation of immune responses by L-arginine metabolism. *Nat. Rev. Immunol.* 5: 641–654.
29. Nahrendorf, M., F. K. Swirski, E. Aikawa, L. Stangenberg, T. Wurdinger, J. L. Figueiredo, P. Libby, R. Weissleder, and M. J. Pittet. 2007. The healing myocardium sequentially mobilizes two monocyte subsets with divergent and complementary functions. *J. Exp. Med.* 204: 3037–3047.
30. Swirski, F. K., M. Nahrendorf, M. Etzrodt, M. Wildgruber, V. Cortez-Retamozo, P. Panizzi, J. L. Figueiredo, R. H. Kohler, A. Chudnovskiy, P. Waterman, et al. 2009. Identification of splenic reservoir monocytes and their deployment to inflammatory sites. *Science* 325: 612–616.
31. Naviliat, M., G. Gualco, A. Cayota, and R. Radi. 2005. Protein 3-nitrotyrosine formation during *Trypanosoma cruzi* infection in mice. *Braz. J. Med. Biol. Res.* 38: 1825–1834.
32. Petray, P., E. Castaños-Velez, S. Grinstein, A. Orn, and M. E. Rottenberg. 1995. Role of nitric oxide in resistance and histopathology during experimental infection with *Trypanosoma cruzi*. *Immunol. Lett.* 47: 121–126.
33. Saftel, M., B. Fleischer, and A. Hoerauf. 2001. Stage-dependent role of nitric oxide in control of *Trypanosoma cruzi* infection. *Infect. Immun.* 69: 2252–2259.
34. Vespa, G. N., F. Q. Cunha, and J. S. Silva. 1994. Nitric oxide is involved in control of *Trypanosoma cruzi*-induced parasitemia and directly kills the parasite in vitro. *Infect. Immun.* 62: 5177–5182.
35. Mori, M., and T. Gotoh. 2000. Regulation of nitric oxide production by arginine metabolic enzymes. *Biochem. Biophys. Res. Commun.* 275: 715–719.